



HAL
open science

Vortex ring state protection flight control law.

B. Dang-Vu

► **To cite this version:**

B. Dang-Vu. Vortex ring state protection flight control law.. 39th European Rotorcraft Forum, Sep 2013, MOSCOU, Russia. hal-01061133

HAL Id: hal-01061133

<https://hal-onera.archives-ouvertes.fr/hal-01061133>

Submitted on 5 Sep 2014

HAL is a multi-disciplinary open access archive for the deposit and dissemination of scientific research documents, whether they are published or not. The documents may come from teaching and research institutions in France or abroad, or from public or private research centers.

L'archive ouverte pluridisciplinaire **HAL**, est destinée au dépôt et à la diffusion de documents scientifiques de niveau recherche, publiés ou non, émanant des établissements d'enseignement et de recherche français ou étrangers, des laboratoires publics ou privés.

VORTEX RING STATE PROTECTION FLIGHT CONTROL LAW

Binh Dang-Vu
ONERA, France – binh.dangvu@onera.fr

Abstract

The current and future trend towards fly-by-wire (FBW) control architectures on helicopters is aimed at bringing improved handling and enhanced safety. By giving a direct input through electrical signals, commands are much more precise enhancing overall safety. Furthermore, the pilot commands are monitored by the FBW control system to ensure the helicopter is kept within the flight protection envelope. As a result, the pilot always can get the maximum performance out of the helicopter without running the risk of exceeding safety margins. Vortex Ring State (VRS) conditions are among adverse flight conditions which mostly occur within a boundary confined to a part of the flight envelope at low forward airspeeds and at steep angles of descent or high rates of descent. The contribution of the present paper is to incorporate VRS boundaries inside a FBW flight control law in order to prevent the helicopter from entering the VRS region. The stability margin given by the heave mode damping is used as a metric to quantify the safety margin. Simulations show the good performance of the VRS-protection function.

1. INTRODUCTION

The integration of civil transport helicopter in the air traffic may be constrained in the future by more severe noise abatement procedures in terminal area operations. One of the most prominent sources of helicopter main rotor noise is Blade-Vortex Interaction (BVI) noise [1]. BVI noise occurs mostly during low/moderate speed descent flight, and sometimes in turning or manoeuvring flight, when the rotating blades pass in close proximity to the previously shed rotor tip vortices [1, 2]. Multi-segment decelerating descent approaches, and particularly steep descents have been shown to be effective in ground noise abatement. However, helicopter flight in steep descent has its undeniable limits, mainly characterized by the behaviour of the main rotor aerodynamics. The settling with power also referred to as Vortex Ring State (VRS) is most likely the first limiting flight regime. Settling with power is a condition of powered flight where the helicopter settles into its own downwash causing severe loss of lift. When the condition arises, increasing the rotor power merely feeds the vortex motion without generating additional lift. Helicopter pilots are most commonly taught to avoid VRS by monitoring their rates of descent at lower airspeeds. When encountering VRS, pilots are taught to apply recovery procedures to fly out of the condition. Various VRS protection flight control systems have been developed. The DLR active side-stick provides force feedback active cues to the pilot from a VRS avoidance function [3, 4]; the VRS limits are

transformed into limits in control deflection and brought to the pilot in the form of soft stops. The Bell Helicopter control system of Ref. [5] delays or prevents VRS by generating oscillatory collective input prior to the onset of the VRS; the control inputs are transient, do not require input from the pilot, and do not affect the flight path of the rotorcraft. With the advent of fly-by-wire (FBW) technology application to future commercial transport helicopter, it is foreseen that an automatic protection of the flight envelope will be required, and VRS conditions are among adverse flight conditions against which the helicopter must be protected. The trend towards FBW control architectures on helicopters is aimed indeed at bringing improved handling and enhanced safety. By giving a direct input through electrical signals, commands are much more precise enhancing overall safety. Furthermore, the pilot commands are monitored by the FBW control system to ensure the helicopter is kept within the flight protection envelope. As a result, the pilot always can get the maximum performance out of the aircraft without running the risk of exceeding safety margins. Previous research at ONERA on VRS has focused on 1/ inflow modelling [6], 2/ experimentation with in-flight rotor flow measurement on the Dauphin 6075 research helicopter in cooperation with CEV, the French Flight Tests Centre [7], 3/ prediction of VRS onset via criteria boundaries [8-11], 4/ protection through active side-stick, in collaboration with DLR [3]. The contribution of the present paper is to develop an automatic flight control law which prevents the helicopter from entering the VRS region. VRS automatic protection is an aerodynamic

protection. The aim of the study is oriented towards protecting future FBW transport helicopter against VRS with the same philosophy as for FBW fixed-wing transport aircraft which pioneered automatic high angle of attack protection. The paper is organised as follows: the following Section 2 presents an alternative approach to those already investigated at ONERA for determining the VRS region. Section 3 presents the development of the flight control law. Section 4 presents simulation results of VRS entry and avoidance scenarios.

2. VRS BOUNDARIES

2.1. Summary of previous research at ONERA

In Ref. [6], ONERA has developed a semi-empirical inflow model suitable for flight dynamics calculations from an improvement of momentum theory solutions in vertical descent and their extension to descending forward flight. Figure 1 shows the mean induced velocity of the rotor for several values of horizontal velocity. The vertical and horizontal velocities are normalized to the ideal induced velocity in hover $V_{i0} = \sqrt{T/2\rho A}$, where T is the rotor thrust ρ the air density and A the rotor disk area.

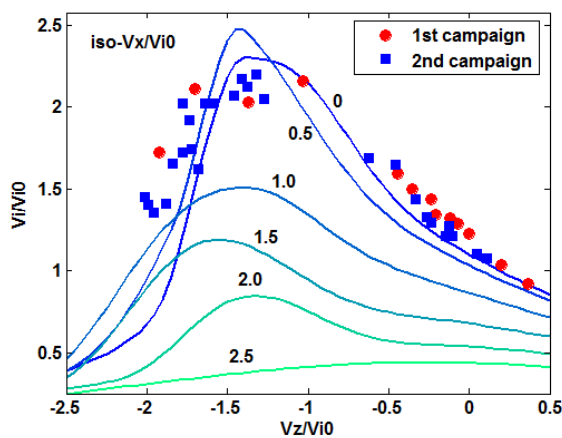


Figure 1: Inflow model for descending forward flight, and experimental data for axial flow [6].

In Figure 1, the results for axial flow obtained from the two flight tests campaigns with the CEV Dauphin 6075 helicopter [7] are also shown. The mean induced velocity of the rotor was estimated from in-flight power measurements [12].

Figure 2 presents VRS boundaries based on the Dauphin 6075 flight tests [7]. Two flight procedures were applied to fly the helicopter into VRS. Procedure (a): from level flight at a given forward velocity, collective input is gradually decreased until

the helicopter enters vortex-state. The manoeuvre is repeated for different forward velocities, determining thus the VRS upper limit. Procedure (b): from a descending flight with fixed vertical speed, the forward velocity is gradually decreased until the VRS is reached. Repeating this operation allows determining the VRS side limit (“knee”). In Figure 2, the vertical velocity drop primarily defines the boundary, but points where fluctuations increase are also shown. Other data available in the literature show a good agreement with the boundary identified from the Dauphin 6075 flight tests. The boundary from the ONERA VRS model is also plotted in Figure 2. This semi-empirical model was developed based on the mean convection of the tip vortices:

$$\sqrt{(V_x/k)^2 + (V_z + V_i/2)^2} \leq \varepsilon \text{ with } k = 4 \text{ and } \varepsilon = 0.1 \text{ for severe fluctuation levels.}$$

The factor k accounts for the tendency of the vortices to stay in the plane of the disk; $(V_z + V_i/2)$ is the average of the vertical velocity inside and outside of the slipstream.

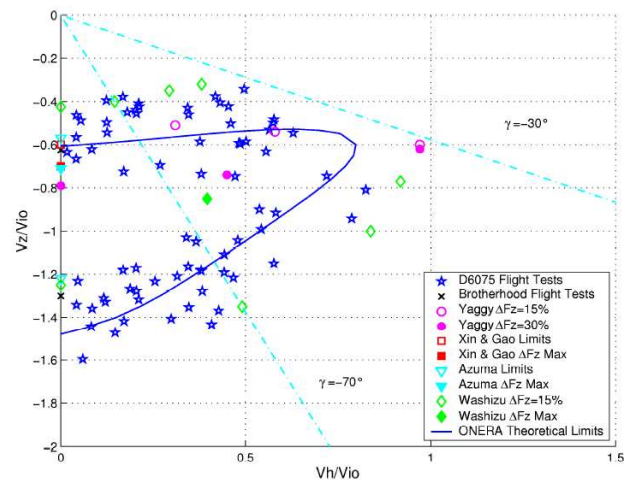


Figure 2: VRS boundaries. Comparison between data and model Ref. [7].

The comparison of the VRS model with the experimental data shows that it gives a good prediction of the VRS. The data of Figure 2 show that VRS cannot be encountered if $V_x > V_{i0}$. Below V_{i0} , the pilot must keep a rate of descent higher than $-0.3 \cdot V_{i0}$ to avoid VRS. A slope angle greater than -30 deg also ensures safe flight.

2.2. VRS boundary based on stability analysis

The aim of the present study is to develop a flight control law ensuring a protection against VRS. While the VRS boundary of Figure 2 gives a prediction of the conditions for entering VRS, the safety margin that a control law must ensure has not been considered yet. Furthermore, as long as flight stability and control is concerned, it is more natural to consider a stability margin directly related to the

eigenvalues of the helicopter dynamics system rather than a safety margin based on the aerodynamic mean convection of the tip vortices defined above by the parameter ε . Therefore, the rotor mean inflow in VRS identified from flight tests (Figure 1) has been implemented in an analysis to calculate the Dauphin 6075 nonlinear flight dynamics. The stability analysis uses a continuation method to calculate the combinations of stabilized forward speed and vertical speed that drive the vehicle into instability. The simulation model is implemented in the HOST code [13] and formulated into a nonlinear dynamical model represented as ordinary nonlinear differential equations:

$$\dot{x} = f(x, \lambda)$$

where x is the n -dimensional state vector, λ is the m -dimensional parameter vector, f is a vector of n nonlinear continuous and differentiable functions.

As opposed to linear systems, a nonlinear differential system may have several asymptotic states for a given set of parameters. In the simplest cases, as generally in flight dynamics, the asymptotic states are fixed points corresponding to the nonlinear equation:

$$0 = f(x, \lambda)$$

In other cases, the asymptotic states are periodic orbits called limit cycles, satisfying:

$$0 = \int_0^T f(x, \lambda) dt$$

with a period T which is an additional unknown.

In the present case, the parameter used in the continuation method is the collective control. The bifurcations encountered in the VRS region are of turning point type, i.e. a real eigenvalue of the Jacobian matrix associated with the linearization about a given equilibrium point crosses the imaginary axis through the origin. At this point a stable solution will suddenly jump to another stable solution. This corresponds to the entry to VRS and the transition to a stabilized windmill-brake regime. The set of bifurcation points, called the bifurcation surface, is then identified as being the VRS boundary. Figure 3 displays the bifurcation surface in the horizontal speed-vertical speed (V_x, V_z) plane, both normalized with hover induced velocity. The flight tests data of Ref. [7] corresponding to VRS entry and VRS exit are also plotted.

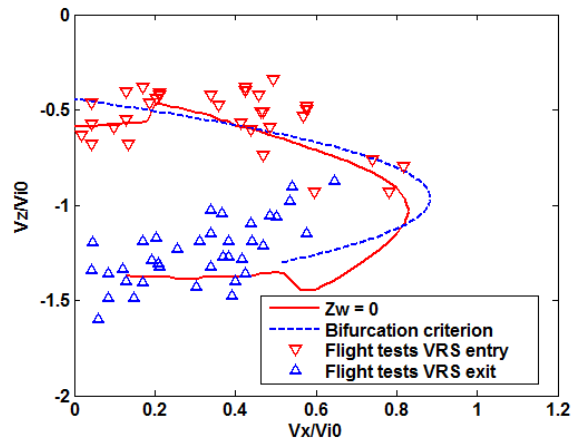


Figure 3: VRS boundary as a bifurcation surface.

The dotted curve is derived from the calculation of the steady state of the full-order system and the eigenvalues of the reduced-order system (u, v, w, V_i), where u, v, w denote the body-axis velocity components and V_i denotes the mean induced velocity [10]. The solid curve is derived from the calculation of the steady state of the full order system and the eigenvalue of the reduced order system (w). In this latter case, the VRS entry is therefore characterized by a heave damping coefficient Z_w crossing zero from negative to positive. Johnson in Ref. [14] used the same stability derivative Z_w to characterize the VRS boundary. The comparison of the VRS boundaries based on stability analysis with the flight tests data shows a correlation of the same order as the boundary based on the mean convection of the rotor tip vortices of Figure 2. The prediction of VRS entry in the “knee” region is better. The slight jump that can be observed on the $Z_w = 0$ boundary at 0.20 normalized horizontal speed is due to the interactions between the main rotor and the horizontal stabilizer which become effective from that forward speed. The other jump at 0.60 normalized horizontal speed is due to the same effects but in the windmill-brake regime. The calculation of the boundary based on the 4th order system (u, v, w, V_i) (dotted curve) did not take into account the rotor-stabilizer interactions [10].

The VRS boundary based on the heave stability derivative Z_w is now verified by means of nonlinear simulations. Figure 4 and Figure 5 present time histories of the helicopter response to a step input on the collective lever. The helicopter is flown initially in a horizontal flight path with a speed of 10km/h. At $t=5s$, the collective lever is lowered by -8% (Figure 4) or -9% (Figure 5) of full-scale deflection.

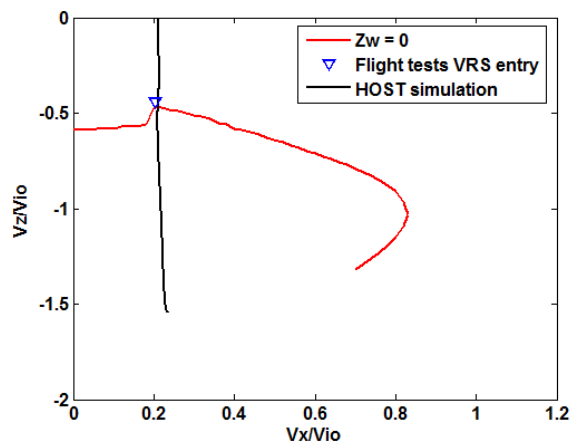
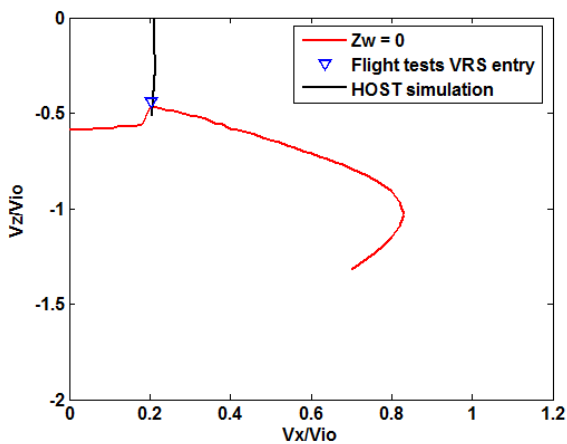
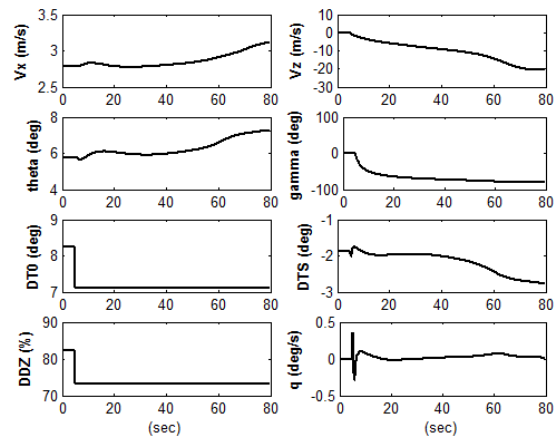
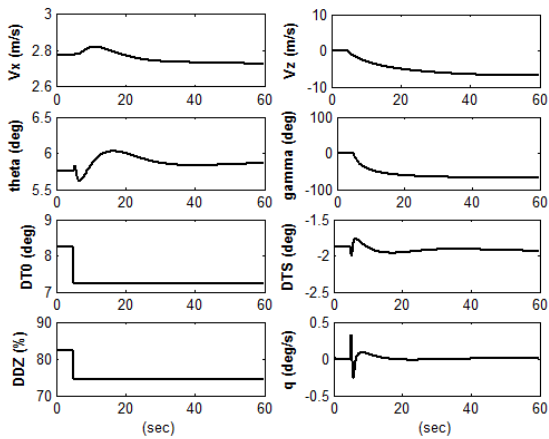


Figure 4: HOST simulation of helicopter almost entering VRS.

Figure 5: HOST simulation of helicopter entering VRS and exiting to windmill-brake state.

On the figures, DDZ denotes the collective lever deflection in percentage of full-scale deflection; DTO, DTS denote collective, longitudinal cyclic pitch angles; q , θ , γ denote pitch rate, pitch attitude, flight path angle. In Figure 4, following the step input on the collective lever, the helicopter is stabilized in a descent with a slope of -68° ; in the (V_x, V_z) plane, the stabilized point is practically on the $Z_w = 0$ curve and it is close to a flight test VRS entry point. In Figure 5, with only 1% of collective increment, the helicopter vertical speed drops to a much lower value, the stabilized slope being equal to -81° . The jump from a steady state close to an experimental VRS entry point to another steady state has been verified for several points along the $Z_w = 0$ curve. This shows that the stability analysis based on the reduced order system is validated by full nonlinear simulations. Any improvement of the VRS prediction should concern mainly the simulation model, and in the first place the inflow model.

The safety margin for an approach-to-VRS can be defined as the distance in the (V_x, V_z) plane of a current point to the bifurcation surface $Z_w = 0$. The stability margin given by the heave damping coefficient Z_w is therefore used as a metric to quantify the safety margin. Figure 6 displays the safety regions delimited by various values of Z_w . Only the upper part of the VRS boundary and the side part (the “knee”) will be of interest, the lower part corresponding to VRS exit to the windmill-brake state is not used to develop the flight control law. Depending on how far a helicopter must avoid VRS, the flight control law must be designed such to keep the heave mode damping coefficient below a negative value to be fixed. This requires obviously a good modelling of the helicopter aerodynamics in the vicinity of the VRS flight regime, in the same way a good modelling of a fixed-wing aircraft in the stall flight regime is needed in order to design an angle of attack protection flight control law.

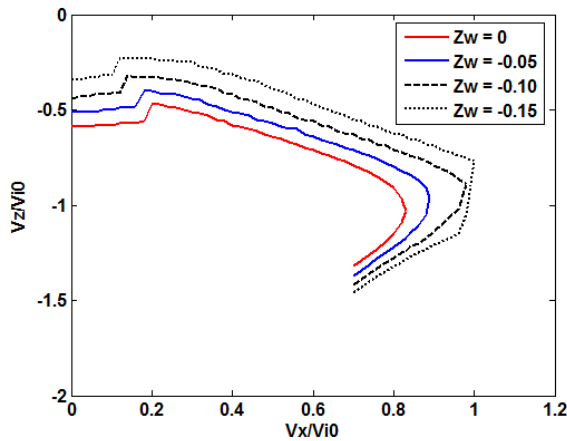


Figure 6: Safety margins based on heave mode damping coefficient.

3. VRS PROTECTION FLIGHT CONTROL LAW

3.1. Control law development

This section describes the design of the VRS protection control law. The design approach consists of the following steps: 1/ selection of the VRS avoidance region in the (V_x, V_z) plane by fixing a safety margin, 2/ current estimation and future prediction of helicopter horizontal and vertical airspeed components, 3/ synthesis of collective and longitudinal cyclic control orders.

Safety margin: As mentioned in the previous section, the safety margin for an approach-to-VRS can be defined as the distance in the (V_x, V_z) plane of a current point to the bifurcation surface $Z_w = 0$. The stability margin given by the heave damping coefficient Z_w is therefore used as a metric to quantify the safety margin and the corresponding curve Z_w is used to delimitate the flight envelope.

Airspeed estimation and prediction: A key parameter for flight condition monitoring is the helicopter airspeed. This is even more crucial for flight conditions close to VRS. Airspeed is normally obtained via pitot-static tubes mounted near the front of the helicopter. If the helicopter is travelling faster than approximately 50km/h, then the speed indication works accurately as the pitot-static tubes are not in the downwash of the rotor system. However, if the helicopter is travelling at less than 50km/h then the pitot-static tubes are within the downwash from the rotor blades giving an error for the airspeed measurement. Methods of determining the helicopter speed at low speed include - mechanical methods such as the LORAS [15] (Low Range Airspeed Sensor) system, the LASSIE [16] (Low AirSpeed Sensing Indication Equipment) system, etc., and - non mechanical methods such as GPS and algorithm methods. In the present study,

estimated current airspeed and predicted airspeed are calculated via a Kalman-Bucy filter hybridizing inertial and air data measured from generic sensors models.

Control law synthesis:

Figure 7 illustrates the logic that activates the VRS protection function of the flight control system when the predicted airspeed over a fixed time horizon penetrates the area delimited by the Z_w stability margin boundary.

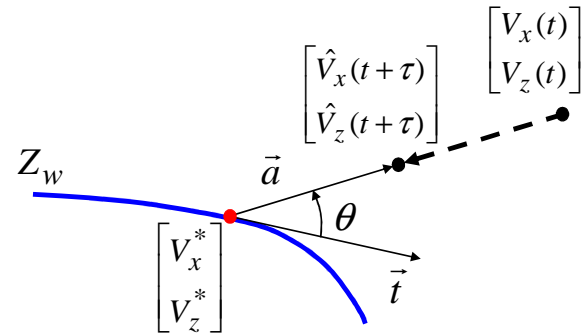


Figure 7: Logic for activating the VRS protection function

Let (V_x, V_z) the current airspeed, (\hat{V}_x, \hat{V}_z) the predicted airspeed at time $t + \tau$, and let (V_x^*, V_z^*) the borderline airspeed defined by the intersection of the line $(\hat{V}_x - V_x, \hat{V}_z - V_z)$ with the boundary. One simple way of finding whether the predicted airspeed is inside or outside the region delimited by the boundary is to calculate the angle between a tangent vector \vec{t} to the boundary and the vector $\vec{a} = (\hat{V}_x - V_x^*, \hat{V}_z - V_z^*)$,

$$\sin \theta = \frac{\|\vec{t} \times \vec{a}\|}{\|\vec{t}\| \|\vec{a}\|}$$

If the predicted airspeed is inside the VRS region, the error between predicted airspeed and borderline airspeed is used to feed the VRS protection control law through a proportional and integral action. A linear model is used to synthesize the control law. The linearized equations of the helicopter dynamics are:

$$\dot{x} = Ax + B(u_{pilot} + u_{sas} + u_{vrs})$$

where x is the state vector, u_{pilot} is the input vector from the pilot, u_{sas} is the input vector from the stability augmentation system (SAS), and u_{vrs} is the input vector from the VRS protection system.

The SAS control law can be expressed as:

$$u_{sas} = Kx$$

Let,

$$\hat{y} = (\hat{V}_x, \hat{V}_z)^T$$

$$y^* = (V_x^*, V_z^*)^T$$

the controlled vector and the objective vector. The error vector is linearized as:

$$\hat{y} - y^* = Cx + D(u_{pilot} + u_{sas})$$

With a proportional integral control law of the form

$$u_{vrs} = K_1(\hat{y} - y^*) + K_2 \int_0^t (\hat{y} - y^*) dt$$

the helicopter dynamics are governed by the following closed-loop system:

$$\frac{d}{dt} \begin{bmatrix} x \\ \int \hat{y} - y^* \end{bmatrix} = \begin{bmatrix} A + BK + BK_1C & BK_2 \\ C + DK & 0 \end{bmatrix} \begin{bmatrix} x \\ \int \hat{y} - y^* \end{bmatrix} + \begin{bmatrix} B + BK_1D \\ D \end{bmatrix} u_{pilot}$$

The modes of the system are determined by the eigenvalues and eigenvectors of the augmented state matrix and they are assigned by choosing appropriately the gain matrices K1 and K2. Figure 8 shows the block diagram of the control system. Collective and longitudinal cyclic orders for VRS protection are generated using acceleration and speed measurement feedback and are added to the actual stabilization orders. The VRS-protection mode is activated when the airspeed predicted over a fixed time horizon penetrates the area delimited by the VRS stability margin boundary.

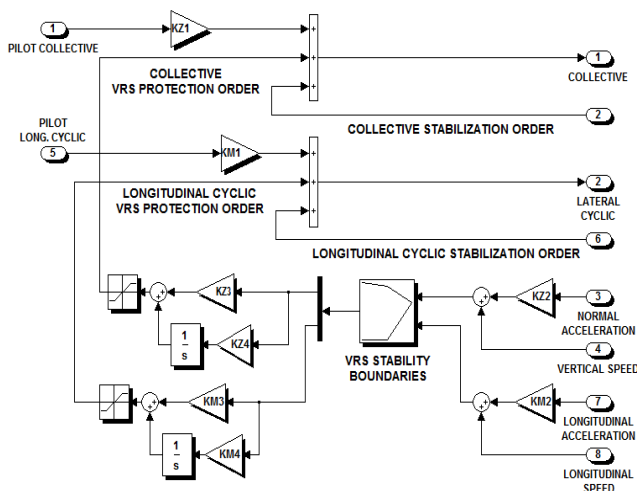


Figure 8: Block diagram of VRS protection control system.

3.2. Simulation results

The two flight procedures that were applied during the flight tests to fly the helicopter into VRS [7] are simulated with the HOST code to verify the performance of the VRS protection control law. Procedure (a): from level flight at a given forward velocity, collective input is decreased until the helicopter enters in vortex-state through the upper part of the boundary. Procedure (b): from a descending flight with fixed vertical speed, the forward velocity is decreased until the VRS is reached by the side part of the boundary.

Procedure (a): The below-illustrated (Figures 9 and 10) are trajectories flown by not protected or protected helicopter, when the pilot applies a collective command to make a steep descent. Initially the helicopter is flown in a horizontal flight path with a velocity of 10km/h. At t=5s, a lower-down is executed by a collective lever DDZ step input of -11% full-scale deflection. Without the VRS protection, the helicopter enters the VRS region by the upper part as illustrated in Figure 9. The helicopter then exits the VRS region to the windmill-brake regime. With the VRS protection, a pull-up order on the collective is generated from t=11.7s in order to keep the flight point on the borderline of the safety region delimited by $Z_w = -0.05$. The graph demonstrates the efficiency of the protection, to ensure a safety margin with respect to the VRS area.

Procedure (b): Figures 11 and 12 display trajectories flown by not protected or protected helicopter, when the pilot applies a longitudinal cyclic command to reduced forward speed. Initially the helicopter is flown in a descent with a horizontal speed of 50km/h and a vertical speed of -13.2m/s. At t=5s, a pull-aft is executed by a longitudinal stick DDM step input of -6% full-scale deflection. Without the VRS protection, the helicopter enters the VRS region by the "knee" as illustrated in Figure 11. To avoid a departure into the windmill-brake regime, a stabilization order in vertical speed is introduced in the collective control. With the VRS protection, a pitch-down order on the longitudinal cyclic is generated from t=9.2s in order to keep the flight point on the borderline of the safety region delimited by $Z_w = -0.05$. The graph demonstrates the efficiency of the protection, to ensure a safety margin with respect to the VRS area.

4. CONCLUSION

The contribution of the present paper is to incorporate VRS boundaries inside a flight control law in order to prevent the helicopter from entering the VRS region. The comparison of the VRS boundaries based on stability analysis with the flight tests data shows a correlation of the same order as

the boundary based on the mean convection of the rotor tip vortices. The stability margin given by the heave mode damping coefficient is used as a metric to quantify the safety margin. The use of this damping coefficient for synthesizing the VRS-protection control law is straightforward. Simulations show the good performance of the VRS-protection control law. The implementation of the VRS protection function in future FBW civil transport helicopter should enable the pilot to get the maximum performance out of the helicopter without running the risk of exceeding safety margins.

REFERENCES

1. Schmitz, F. H. and Yu, Y. H., "Helicopter Impulsive Noise: Theoretical and Experimental Status", *Journal of Sound and Vibration*, Vol. 109, No. 3, pp. 361-422, 1986.
2. Yu, Y., "Rotor Blade-Vortex Interaction Noise." *Progress in Aerospace Sciences*, Vol. 36, pp. 97-115, 2000.
3. Abildgaard, M., Binet, L., von Grünhagen, W., and Taghizad, A., "VRS Avoidance as Active Function on Side-Sticks", in *American Helicopter Society 65th Annual Forum Proceedings*, Grapevine, Texas, May 27-29, 2009.
4. von Grünhagen, W., Müllhäuser, M., Abildgaard, M., Lantzsch, R., "Active Inceptors in FHS For Pilot Assistance Systems", *36th European Rotorcraft Forum*, Paris, France, Sep 7-9, 2010.
5. Kisor, R.L., "Control System for Rotorcraft for Preventing the Vortex Ring State", *Bell Helicopter Textron Inc.*, Patent No. US 6880782 B2, April 2005.
6. Jimenez J., Desopper A., Taghizad A., Binet L., "Induced Velocity Model in Steep Descent and Vortex-Ring State Prediction", in *27th European Rotorcraft Forum 2001 proceedings*.
7. Taghizad, A., Jimenez, J., Binet, L., and Heuzé, D., "Experimental and Theoretical Investigation to Develop a Model of Rotor Aerodynamics Adapted to Steep Descents", in *American Helicopter Society 58th Annual Forum Proceedings*, Montreal, Canada, June 11-13, 2002.
8. Jimenez, J., "Experimental and Theoretical Study of the Behaviour in Steep Descent Helicopter: Modelling of the Vortex Ring State", Ph.D. Dissertation, University of Marseille, December 2002.
9. Basset, P.M., and Prasad, J.V.R., "Study of the Vortex Ring State Using Bifurcation Theory", in *American Helicopter Society 58th Annual Forum Proceedings*, Montreal, Canada, June 11-13, 2002.
10. Kolb, S., "Théorie des bifurcations appliquée à l'analyse de la dynamique du vol des hélicoptères", *Thèse INP Grenoble*, Juin 2007.
11. Basset, P.M., Chen, C., Prasad, J.V.R., and Kolb, S., "Prediction of Vortex Ring State Boundary of a Helicopter in Descending Flight by Simulation", in *Journal of the American Helicopter Society*, 2008, pp. 139–151.
12. Jimenez J., Taghizad A., Arnaud A., "Helicopter Flight Tests in Steep Descent: Vortex-Ring State Analysis and Induced Velocity Models Improvement", *CEASTRA3*, 2002.
13. Benoit, B., Dequin, A.-M., Basset, P.-M., Gimonet, B., von Grünhagen, W., Kampa, K., "HOST- A General Helicopter Simulation Tool for Germany and France", *56th American Helicopter Society Annual Forum*, 2000.
14. Johnson, W., "Model for Vortex Ring State Influence on Rotorcraft Flight Dynamics", *NASA TP-2005-213477*, Dec. 2005.
15. Abbot, W.Y., Boirun, B.H., Hill, G.E., Tavares, E.J., "Flight Evaluation Pacer Systems Low-Range Airspeed System LORAS 1000", *USAAEFA Project No. 75-17-1*, May 1977.
16. Kaletka, J., "Evaluation of the Helicopter Low Airspeed System LASSIE", *J. American Helicopter Society*, vol. 28, no. 4, pp. 35-43, Oct. 1983.

COPYRIGHT STATEMENT

The authors confirm that they, and/or their company or organization, hold copyright on all of the original material included in this paper. The authors also confirm that they have obtained permission, from the copyright holder of any third party material included in this paper, to publish it as part of their paper. The authors confirm that they give permission, or have obtained permission from the copyright holder of this paper, for the publication and distribution of this paper as part of the ERF2013 proceedings or as individual offprints from the proceedings and for inclusion in a freely accessible web-based repository.

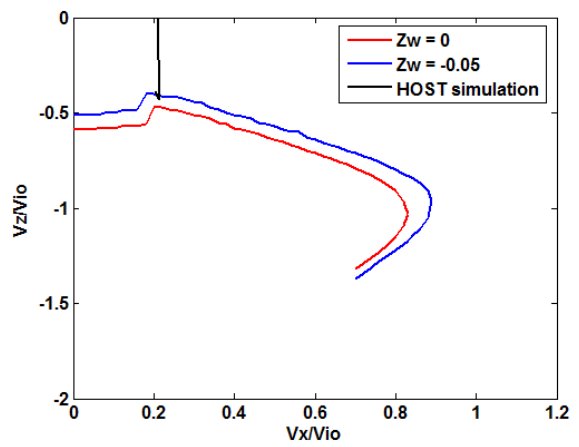
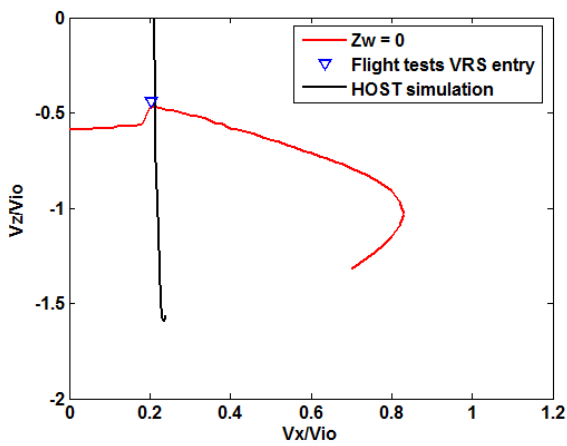
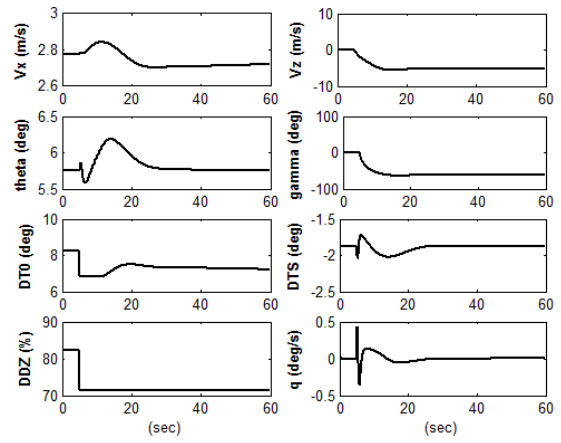
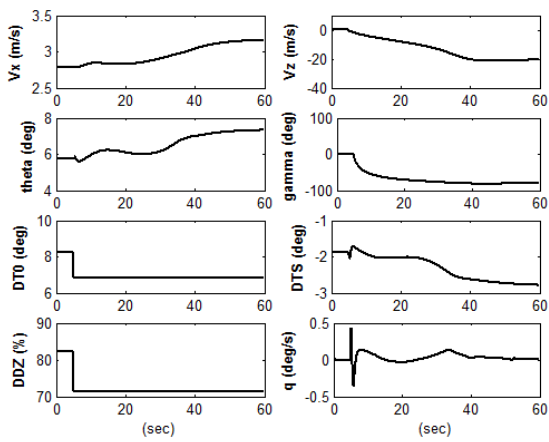


Figure 9: Response to collective step input without VRS protection.

Figure 10: Response to collective step input with VRS protection.

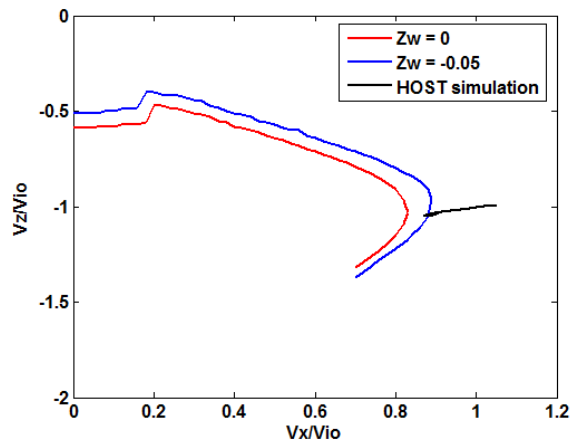
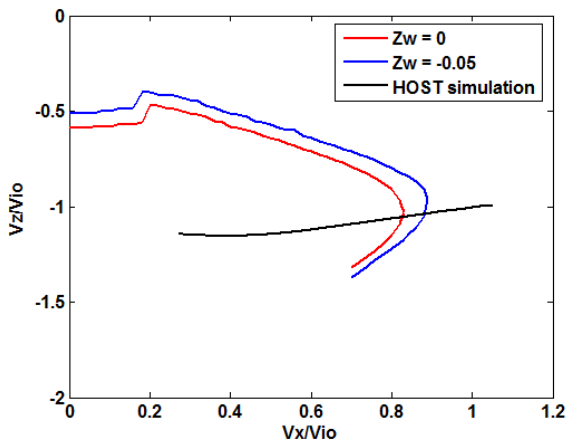
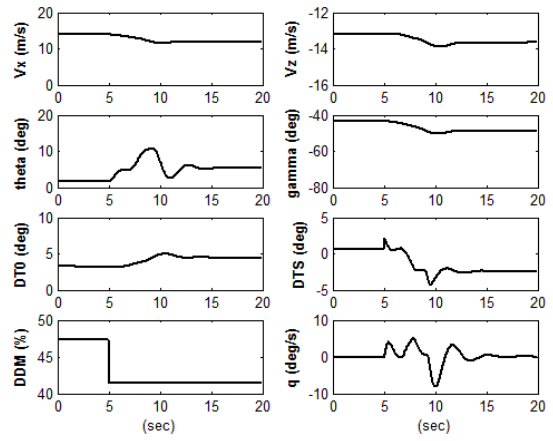
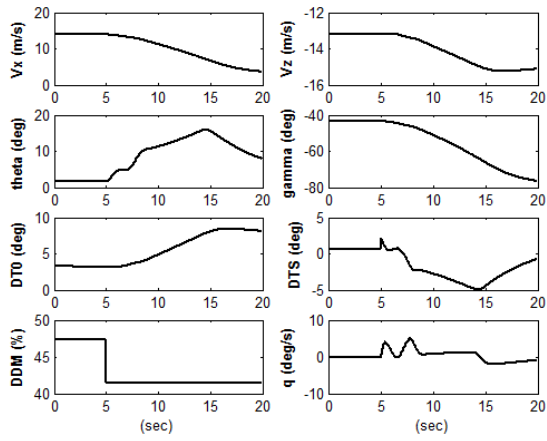


Figure 11: Response to longitudinal cyclic step input without VRS protection.

Figure 12: Response to longitudinal cyclic step input with VRS protection.